Estudios Geológicos
julio-diciembre 2016, 72(2), e051
ISSN-L: 0367-0449
doi: http://dx.doi.org/10.3989/egeol.42328.394

Mapping and analysis of geological fractures extracted by remote sensing on Landsat TM images, example of the Imilchil-Tounfite area (Central High Atlas, Morocco)

Análisis de fracturas geológicas extraídas por teledetección en imágenes Landsat TM, ejemplo de la zona de Imilchil-Tounfite (Alto Atlas central, Marruecos)

H. El Alaoui El Moujahid[1], H. Ibouh[1,2], A. Bachnou[1], M. Ait Babram[3], A. El Harti[4]

[1] Cadi Ayyad University, Faculty of Sciences and Techniques, Marrakesh, Geosciences and Environment Laboratory, Bd A. Khattabi, BO.549, 40000 Guéliz, Marrakesh, Morocco. Email: h.ibouh@uca.ma
[2] LMI_TREMA_IRD, Cadi Ayyad University, Bd. My Abdellah, BO 2390, 40000 Marrakech, Morocco.
[3] Mathematic and Population Dynamic Laboratory; Department of Mathematics, Faculty of Science and Techniques, Marrakech, Bd A. Khattabi, BO 549, 40000 Guéliz, Marrakesh, Morocco.
[4] Moulay Slimane University, Faculty of Sciences and Techniques, Lab. Remote Sensing and GIS applied to Geosciences and Environment, BO: 523 Beni Mellal, Morocco.

ABSTRACT

The use of remote sensing, in this research, can be summarized in mapping and statistical studies of lineaments on the satellites images of the Jurassic outcrops in the Imilchil-Tounfite area, Central High Atlas of Morocco. This is to apply various manual techniques for extracting lineaments from Landsat TM image. Analytical techniques used in this work are: the principal component analysis (PCA) applied to selective bands of the visible and infrared, which allows creating new images with better visual interpretation. Directional filters N0°, N45°, N90°, and N135° with a 5×5 matrix were used to enhance lineaments in the corresponding perpendicular directions, and therefore to obtain a good discrimination of those structures. Preliminary results highlight a dominant geological fracturing trending ENE/WSW with 52% of the total lineaments, a second fracture trending is WNW/ESE at 23%, a third fracture series trending NE/SW with 20% and finally, a minor series of fractures trending NW/SE with 5% of the total lineaments. Distribution and statistical relationship, between fractures and the affected surface on the one hand and the fracture length on the other hand, shows a network of well-structured fractures. The final lineament map constitutes a contribution to complete the geology and assisting the mining and hydrogeological prospection, in the Imilchil-Tounfite area.

Keywords: Remote sensing; lineaments; fractures; Imilchil-Tounfite; High Atlas; Morocco.

RESUMEN

En este trabajo se han aplicado metódos estadísticos de datos obtenidos por teledetección, para la cartografía de lineamientos en afloramientos del Jurásico en la zona de Imilchil-Tounfite, Alto Atlas Central de Marruecos. Las técnicas analíticas utilizadas incluyen el análisis de componentes principales (PCA) aplicado a las bandas visible y infrarrojos, que permite crear nuevas imágenes con una mejor interpretación visual, y filtros direccionales

Recibido el 20 de noviembre de 2015 / Aceptado el 18 de marzo de 2016 / Publicado online el 23 de noviembre de 2016

Citation / Cómo citar este artículo: H. El Alaoui El Moujahid, et al. (2016). Mapping and analysis of geological fractures extracted by remote sensing on Landsat TM images, example of the Imilchil-Tounfite area (Central High Atlas, Morocco). Estudios Geológicos 72(2): e051. http://dx.doi.org/10.3989/egeol.42328.394.

N0°, N45°, N90° y N135° con una matriz de 5×5 para mejorar rasgos en las direcciones perpendiculares correspondientes y obtener una buena discriminación de esas estructuras.

Los resultados preliminares ponen de manifiesto una fractura geológica dominante de tendencia ENE-SW con un 52% del total de lineamientos, una segunda tendencia ONO-S (23%), una tercera serie de fracturas orientada NE-SW (20%) y, por último, una serie de menor importancia de fracturas tendencia NW-SE (5%). Las relaciones estadísticas entre las fracturas y la superficie afectada por un lado y la longitud de la fractura, por otra parte, muestra una red de fracturación bien estructurada. El mapa final de lineamientos constituye una contribución para completar la geología de la zona y como ayuda a las prospecciones mineras e hidrogeológicas en la zona de Imilchil-Tounfite.

Palabras clave: Teledetección; Lineamientos; Fracturas; Imilchil-Tounfite; Alto Atlas; Marruecos.

Introduction

The use of satellite imagery in the Imilchil-Tounfite area Central High Atlas is relatively recent. All the anterior research done in this area is a structural, sedimentary and petrography geology (Frizon de Lamotte *et al.* 2008; Bougadir & Bouabdelli, 1994. Ibouh *et al.,* 1994, Fadile; 2003). Due to its semi-arid climate which is marked by large variations in temperature, severe summer drought and some areas which are characterized by a high altitude (3200m) with a very difficult accessibility, mapping lineaments by conventional methods is insufficient and relatively expensive methods and also takes a lot of time to browse all the field. Thus we use Geographic Information System (GIS) and remote sensing for the establishment and updating of structural maps. Indeed, remote sensing is a discipline that focuses on the analysis of the information carried by electromagnetic radiation reflected and emitted by the Earth's surface, then captured remotely by airborne or space-based instruments. Remote sensing with its synoptic view along with the improvement in spectral and spatial resolution as sensors allows not only the study of a large geographical area, but also accuracy in geological analysis. It permits also to complete some geological contours or some faults not observed previously in the field. The realization of the fault network map and its statistical study gives us a general idea of the spatial behavior of these fractures in the area. Combining inventory lineaments on satellite imagery, along with the auxiliary data and field work allows to have the map fractures and to understand the geological structures of the studied area (Pepe *et al*., 1997; Kavak, 2005). The main objective of this work is to complete the structural mapping in the Imilchil-Tounfite region using remote sensing, which will have a major interest in economic geology (mineral and hydrogeological explorations).

Presentation of studied area

The Imilchil-Tounfite area is located in the Central High Atlas of Morocco, between 5° and 6°W longitude and between 32° and 32° 30'N latitude (Fig. 1). This area shows a geological setting with a lateral succession of anticline ridges; trending N70 (Laville, 1988). The main ridges are those of Tassent, Tasraft, Tirghist, Anfgou, Amagmag and Ait Ali Ouikkou (Fig. 1). These ridges are frequently cored by Jurassic magmatic rocks, including gabbro and troctolites. The anticlines ridges are a result of halokenitic evolution coupled to strike slip structural context during Jurassic time and superposed by alpine deformations later (Michard *et al*., 2011, Ibouh *et al*., 2014), All the anticline ridges are trending between N60 to N90, their structural evolution in the left strike slip context gives a distortion of ridges periclinal ending. So this later confers at the most part of ridges a sigmoid morphology (Fig. 1). (Ibouh, 1995; Ibouh *et al*., 2001; Michard *et al*., 2011).

Materials and methods

Materials

The main material used in this study is the Landsat TM (Thematic Mapper) satellite image of L5201038_03820091111 scene, acquired on 12-31th-2009 (path 201; row 38) Free Download from http://glovis.usgs.gov. This satellite image shows 7 spectral bands (Fig. 2) with 30 m spatial resolution, except the thermal band (band number 6) which has a ground resolution of 120 m.The image can provide to the interpreter, a multitude of structural information's (Semere & Woldai 2006; Kavac, 2005; Qari, 2011). The mapping lineaments needs, besides satellite image, to take account of the topographical map in order to eliminate lineaments related to the human activities (road, railway…). Then geological map

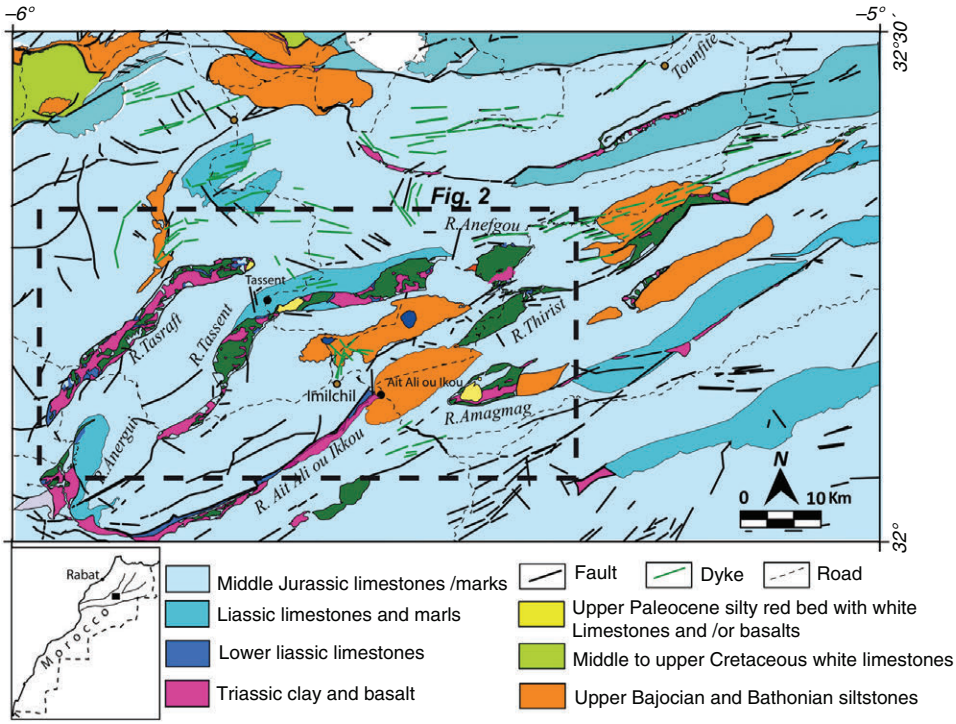

Fig. 1.—Geological and location map of the Imilchil-Tounfite area.

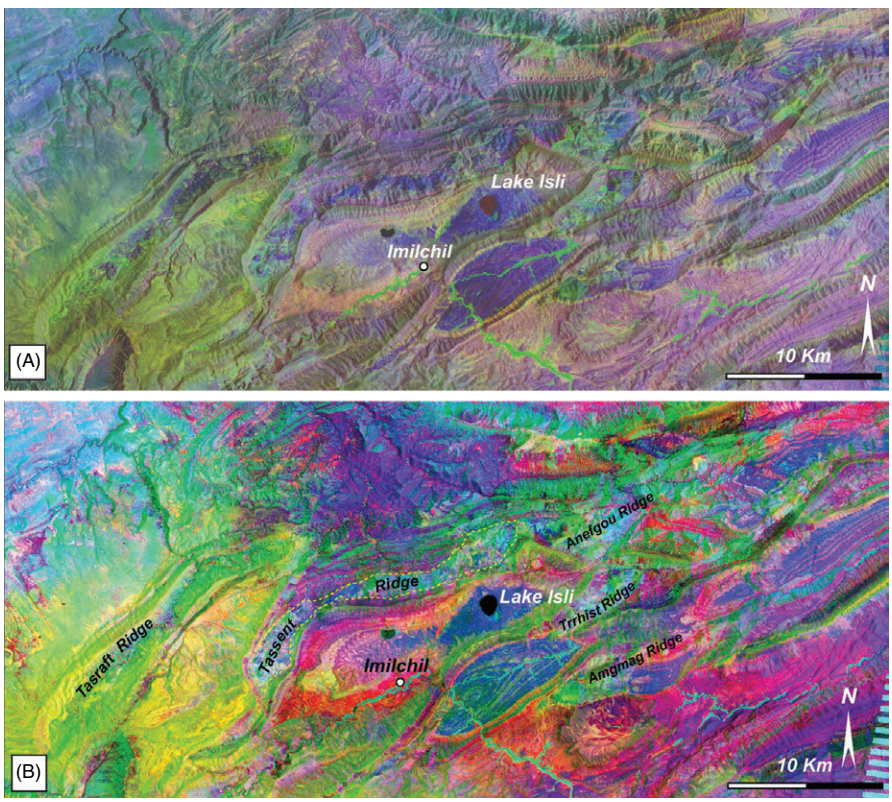

Fig. 2.—Satellite image TM Landsat of the Imilchil-Tounfite area; A: false color composite in RGB (R = 2, G = 4, B = 6); B: false color composite in RGB of the components principal analysis bands (R = PCA1, G = PCA2, B = PCA3).

Table 1.—**Correlation matrix of Landsat TM bands image**

Bands	1	2	3	4	5	6	7	Moyen	Ecart
1	1.00	0.93	0.96	0.79	0.80	0.71	0.83	40.06	30.77
2	0.93	1.00	0.98	0.88	0.92	0.72	0.94	29.62	25.41
3	0.96	0.98	1.00	0.86	0.88	0.72	0.90	22.32	18.02
4	0.79	0.88	0.86	1.00	0.93	0.71	0.90	33.24	27.56
5	0.80	0.92	0.88	0.93	1.00	0.67	0.98	58.80	51.39
6	0.71	0.72	0.72	0.71	0.67	1.00	0.68	85.95	64.74
7	0.83	0.94	0.90	0.90	0.98	0.68	1.00	34.98	30.83

data will be confronted to the lineaments image to give them geological significance.

Data processing methods

The more conventional and most used methods in many studies for the lineaments extraction are the principal component analysis (PCA) as well as the enhancement by spatial filtering. (Amri *et al*., 2011; Aouragh *et al*., 2012; Kassou *et al.*, 2012).

Principal Component Analysis

Principal components analysis or Hotelling transform is an image enhancement technique, based on a mathematical transformation, which reduces the dimensionality of data and segregates noise components (Singh & Harrison 1985). The choice of channels TM sensors was done in order to avoid redundancy and to maximize the quantity of information on the image bands. The analysis of the correlation matrix bands (Table 1) shows high correlations between the visible spectral bands (TM1, TM2 and TM3) and also between the infrared bands (TM4, TM5 and TM7). So the first three principal components analysis of the false color composed images of these correlated bands (images 123 and 457) allows the condensation of High quality information on the distribution of geological features in the area of study. This process allows us to make fine geological interpretations realizing a selective Principal Component Analysis PCA (PCA_{123} and PCA_{457}).

Spatial filters

In order to enhance fractures and faults on the image, directional filters are used for lineaments extracting. Different sizes of matrix filters are applied (3×3; 5×5 and 7×7). The obtained results indicate that those of 5×5 filter size was giving the best and really lineaments which most closely resembles the geological structures in the field. At the end, directional filters (5×5) at 0°N, 45°N, 90°N and 135°N were applied (on a new false color composed image from CPA bands as : PCA_{123} and PCA_{457}) in this work. The 5×5 filter used in this processing image is an edge detection filter. The 5×5 weights of the directional filter for the direction 90°N is given in the table 2.

Table 2.—**Matrix of weighting coefficients of the 5×5 directional filter for N90**

-1	-1	-1	-1	-1
-1	-1	-1	-1	-1
0	0	0	0	0
1	1	1	1	1
1	1	1	1	1

Results and analysis

Mapping discontinuities image

The application of directional filter with 5×5 matrix size on the first bands of PCA_{123} and PCA_{457}, which were used as input images, allows highlighting the lineaments in the study area. These filters provide images in grayscale, where the lineaments based on the selected direction appear brighter than other entities. The maps of discontinuities images were realized by manual extraction (Fig. 3 A, B and Fig. 4 A, B) The lineaments are often enhanced perpendicular to the direction of the selected filter trend.

Lineaments analysis

When applying the directional filter, directional gradients enhance all discontinuities images corresponding to any lithological discontinuity (contact between

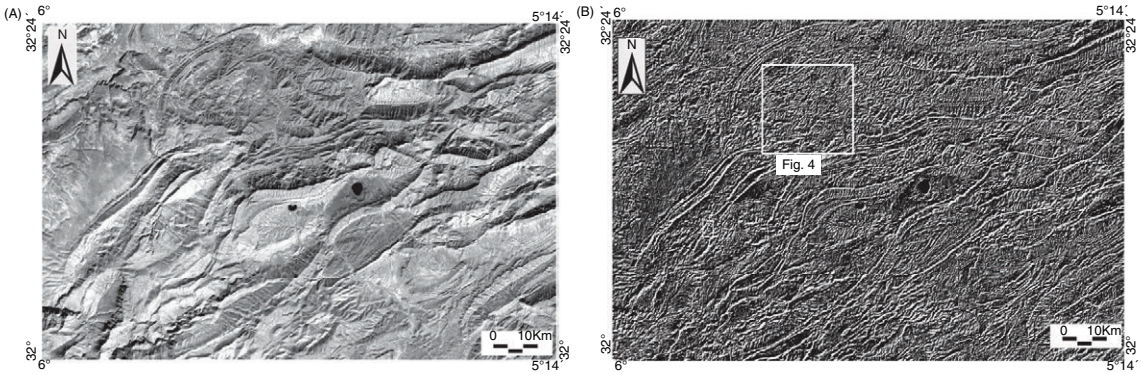

Fig. 3.—A: CPA1 of visible TM Landsat image; B: resulted image after NE directional filter treatment applied on CPA1.

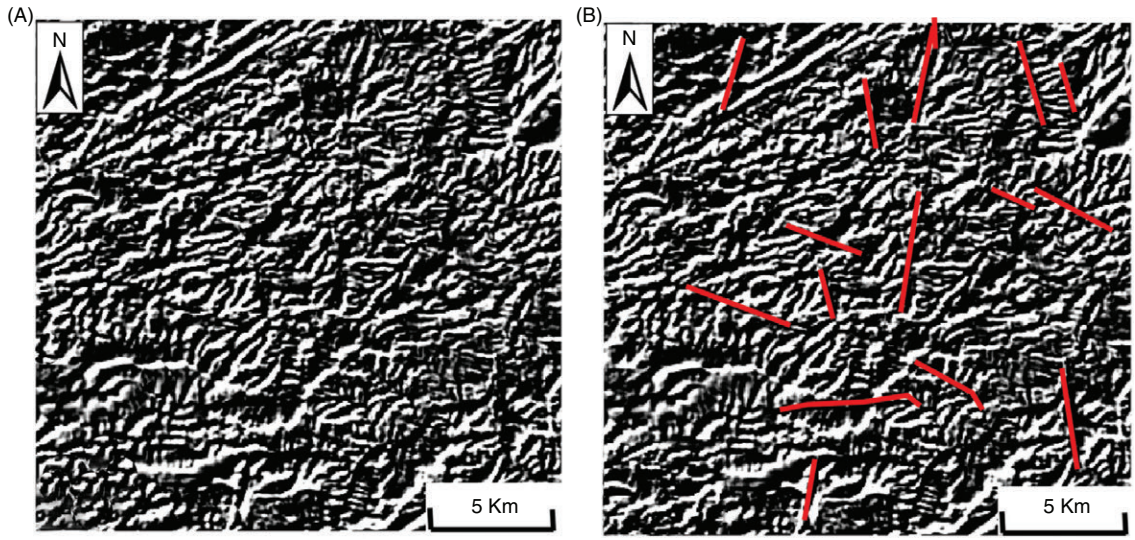

Fig. 4.—A: Enlarged extract from NE directional filter image (see Fig. 3 B for location). B: interpreted fractures on the fig. 4 A image.

different lithological units) and/or structural discontinuity (fault, fracture and joint). In order to give significance to the structural lineaments extracted by remote sensing, the map of discontinuities images is confronted with auxiliary data (geological map, topographic map and field's observations) in order to remove lithological discontinuities, the ridge and crest lines and the anthropogenic lineaments (bitumen road, railway...). The resulted map at the end of all those operations shows a maximum of the fracture and structural lineaments in the study area (Fig. 5 A). Finally some fractures mapped by remote sensing were validated in the field (Fig. 6).

The fractures mapped by conventional methods on the geological map have been reproduced and analyzed (Fig. 5 B). The comparison of the map fractures resulting from remote sensing to those of the geological map shows two main differences: the first one concerns the density of fractures. Those extracted by remote sensing are numerous and denser than those of the conventional mapping in the geological map (sheets of Imilchil and Tounfite 1/100000, Fadile 2003). The second difference concerns the trend of lineaments. Those extracted from satellite image, show a major group of fractures trending N70 to N80 (Fig. 5 A and C), whereas the geological map shows NE-SW trending fractures as major trending lineaments (Fig. 5 B and D). The Interpretation of lineaments extracted by remote sensing on Landsat TM satellite image has revealed the main major faults recognized on the structural map of the Imilchil-Tounfite area and in the field (Fig. 6). At the end, we may conclude that remote sensing by its lineaments extraction methods

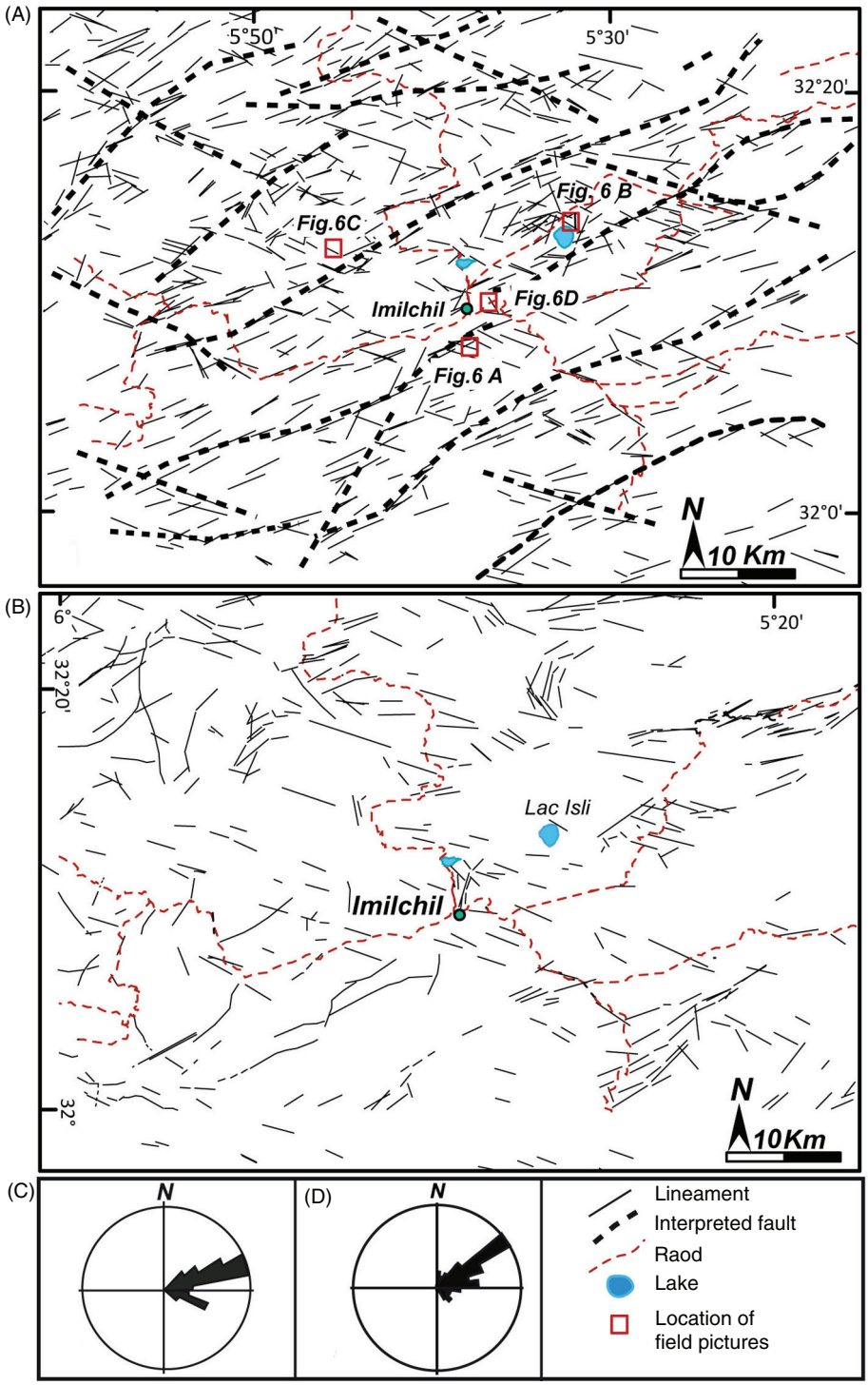

Fig. 5.—A: Fracture map of Imilchil-Tounfite area extracted from Landsat TM image in this work; B: fault map of the Imilchil-Tounfite area extracted from existing geological map. C: Directional rose of mapped faults in the existing geological map D: Directional rose of extracted lineaments by remote sensing methods in this work.

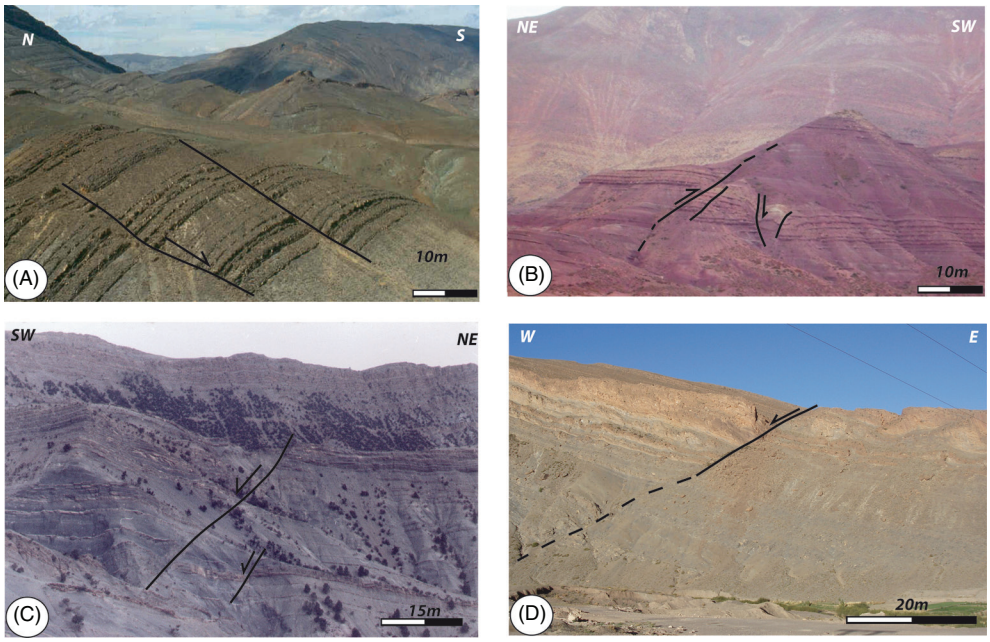

Fig. 6.—Some Fault field pictures corresponding to the lineaments detect by remote sensing. A: Fault NW-SE in the south of Ait Ali ou Ikkou ridge; B: Fault NS to NW-SE in the Bathonian red bed; C: Fault NW-SE in the north of Tassent ridge in the Upper Toarcian marls; D: Normal fault trough the Bajocian limestones in the south east of the Imilchil village (See Fig. 5 for location).

on the TM Landsat image can contribute fully to improve geological maps and complete the geological structure of the study area.

Geostatistics

Geostatistics is used for estimation and prediction of a spatially continuous phenomenon, using data obtained at a limited number of spatial locations (Diggle & Ribeiro, 2007). The geostatistical study of lineaments has been used widely in many researches (Katsuaki & Yuichi 2006; Chiles, 1998; Koike & Komorida, 2001). It allows to understand and to estimate the spatial variability of the phenomenon under study (Gringarten & Deutsch 2001). This mathematical discipline developed from the recognition that the elements studied are not always randomly distributed in space, but may have a degree of spatial correlation known as "structure" (Castaing *et al*., 1988).

The aim of geostatistical study, in this work, fits into a general problematic of characterization, interpretation and valuation of structural lineaments. We used this technic to characterize the spatial dispersion of trend and lengths of fractures in the Imilchil-Tounfite area, central high Atlas of Morocco.

Lineaments variogram analysis

The variograms of fractures distribution in Imilchil-Tounfite region were calculated from cumulative lengths by units of 200 km^2 for each directional series of fractures and the regionalization parameters are determined using spherical and exponential theoretical models. A first analysis of different variograms shows that the fractures, of Imilchil-Tounfite area, are not randomly distributed in space, but have a degree of spatial correlation known as "structure". This structure has range of influence up to 65 km (Fig. 7 A, B and C).

Statistical study

Spatial arrangement

After extraction of the Imilchil-Tounfite fractures on satellite images, the resulting network is described by 10 properties (known as variables). Only implementation of the PCA statistical method will bring out the organization of the network in space. The variables used in PCA study are: 1) the latitude of the fractures and 2) longitude of fractures (Lambert coordinates X and Y positioning in space);

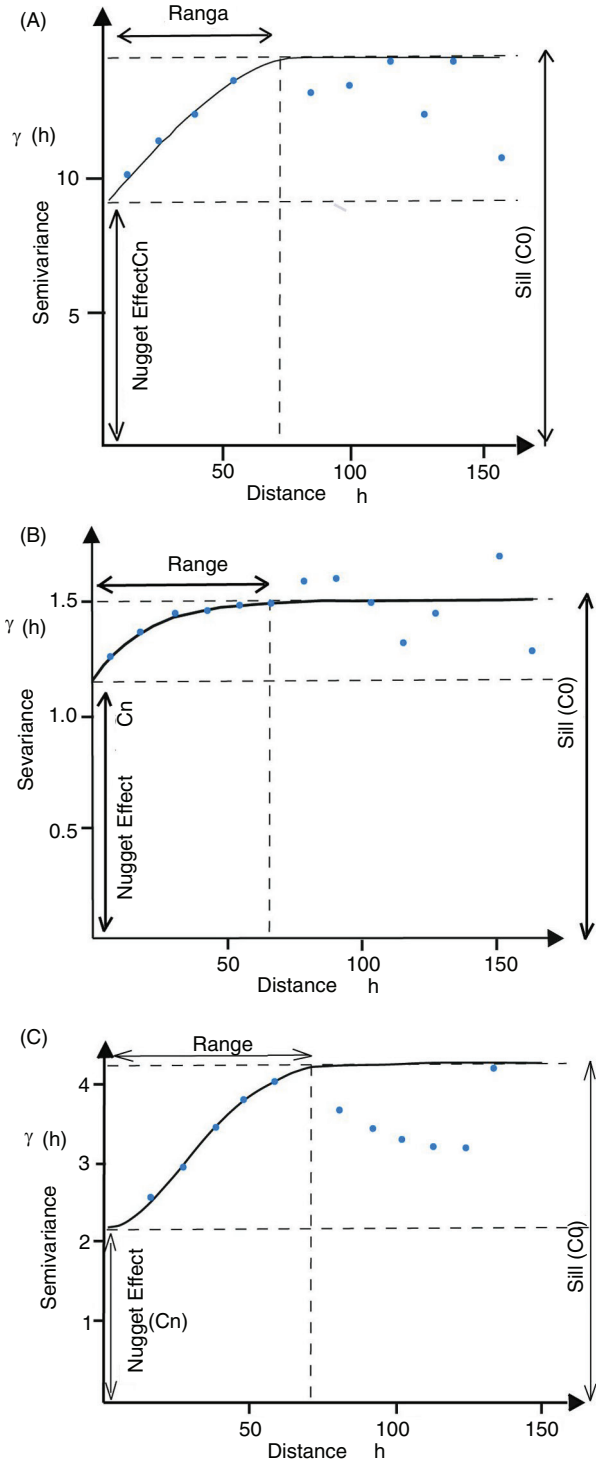

Fig. 7.—Resulting graph from lineament geostatistical study on the Imilchil-Toufite area; A: Variogram fractures all azimuths adjusted by a Spherical model B: Variogram WNW/ESE trends lineaments adjusted by an exponential model. C: Variogram ENE/WSW trends lineaments adjusted by spherical model.

3) the ENE / WSW trend; 4) the WNW / ESE; 5) the NE / SW; 6) NW / SE; 7) the length of ENE / WSW fractures; 8) the length of WNW / ESE fractures; 9) the length of fractures trending NE / SW and 10) the length of fractures trending NW / SE.

The result of the lineaments network study, by the PCA, allowed to calculate 10 principal components with a great percentage of the variance estimated at 56,319 within the three first principal components (CPA_1=21,39; CPA_2=19,29; CPA_3=15,63) (Table 3).

This study also allowed to extract the sum of the square of the selected factors in tow first components (CPA_1=21,397 and CPA_2=40.627) (Table 4) and calculating the sum of the square of the selected factors for rotation for the same components (CPA_1=20,999 and CPA_2=40,687) (Table 5).

The statistical principal component analysis study improves information about the spatial relationships between different lineaments groups trend. According to the Figure 8A, on a grid of 20 km length and 10 km width we find that the ENE-WSW (D1) and WNW-ESE (D2) lineaments are scattered and not coexist in

Table 3.—**Eigen values of the principal component analysis of the lineaments network in the Imilchil-Tounfite area**

	Initial Eigen values		
Component	Sum	% variance	% cumulative
1	2,140	21,397	
2	1,929	19,290	
3	1,563	15,632	56,319
4	1,297	12,969	69,297
5	0,997	9,965	79,252
6	0,866	8,657	87,909
7	0,389	3,891	91,800
8	0,298	2,978	94,778
9	0,270	2,704	97,483
10	0,252	2,517	100,00

Table 4.—**Extraction sum of the square of the selected factors of the lineaments network in the Imilchil-Tounfite area**

	Eigenvalues	extraction sum of the square of the selected factors		
Component	% cumulative	Sum	% variance	% cumulative
1	21,397	2,140	21,397	21,397
2	40,687	1,929	19,290	40,627

Table 5.—**Sum of the square of the selected factors for rotation of the lineaments network in the Imilchil-Tounfite area**

	sum of the square of the selected factors for rotation		
Component	% cumulative	% variance	% cumulative
1	2,100	20,999	20,999
2	1,969	19,688	40,687

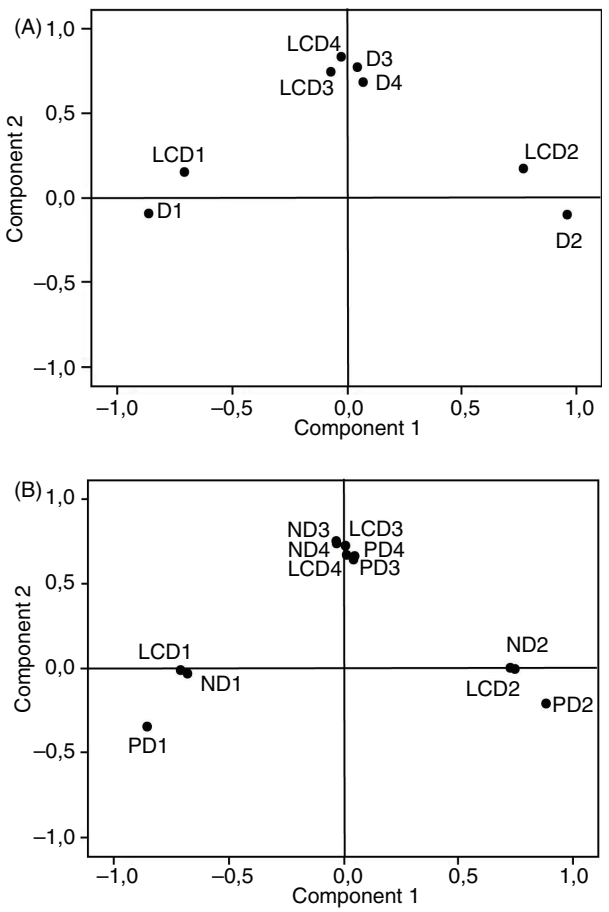

Fig. 8.—Diagram of the principal components distribution of the Imilchil-Tounfite fractures in space after rotation; A: with cumulated length (LCD) depending on the direction of fractures (D1, D2, D3 and D4) B: Cumulated lengths (LCD) and percent (PD) and fractures number (ND of each directions ((D1, D2, D3 and D4). With D1=ENE-WSW; D2=WNW-ESE; D3=NE-SW and D4=NW-SE.

the space. However NE-SW (D3) and NW-SE (D4) coexist within the same location. In order to confirm this conclusion, another statistical study was done as principal component, and taking account the cumulated lengths and the number of fractures in each directions (Fig. 8 B). This study gives a distribution of fractures group as seeing in the figure 8 A.

Lineaments length analysis

Analysis of the lineaments length shows a variation from 500 m to 12 km. The lengths of 374 lineaments mapped by Landsat remote sensing are distributed in 21 classes in steps of 500 m (Fig. 9). For simplicity, they can be grouped into three classes: a main class (75.66%) which includes lineaments whose lengths are between 0.5 and 4 km, followed by a second class (22.19%) of lineaments which have lengths between 5 km and 7 km and at the end a minority class (2.15%) with lengths greater than 7 km.

Interpretation

The digital processing of Landsat TM satellite image and the Geographic Information System (GIS) were used to create a fracture map of the Imilchil-Toufinte Area in the central High Atlas of Morocco. The statistical analysis of faults network, frequency diagram shows clearly that all trends are organized into four main groups (Fig. 5 C): ENE/WSW, WNW/ESE, NE/SW and NW/SE.

The principal component analysis study revealed that the four trend groups of fractures have particular space distribution. Thus the two groups trending ENE/WSW and WNW/ESE cannot coexisting in space of 200 Km square. The two other groups trending NW/SE and NE/SW, are coexisting in the field. This spatial relationship is also visible on the geological map (Fig. 1 and Fig. 5 B), the dispersed directions are the main faulted anticlinal ridges and major faults of the Imilchil-Tounfite area (Interpreted faults in fig. 5 A).They are dispersed because they are separated by wide synclines (10 to 20 Km). However coexisting directions are shown on the geological map (Fig. 1) on the middle part of synclinal form as a short and conjugate strike-slip fault.

The fracture length analysis shows three main groups, the first one is between 0.5 and 4 km (75.66%), the second is between 5 and 7 km (22.19%), and finally a third group is with length greater than 7 km (2.15%). The lineaments lengths distribution corresponds perfectly to the geological map of the study

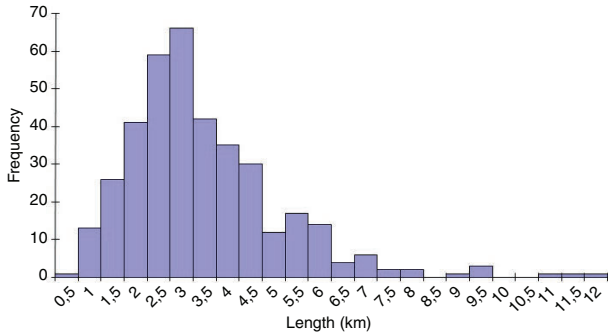

Fig. 9.—Histogram showing the frequency by length of the Imiclhil-Tounfite fractures extracted by remote sensing.

area (Fig. 1 and Fig. 5A). We observed that the longest faults are the rarest (Fig. 1 and fig. 5 A)

The geostatistical study shows that the fracture system plotted from satellite imagery is not randomly distributed in the area, but it has a structured occurrence. The fractures have a degree of spatial correlation known as "structure" with ranges of influence up to 65 km. That is to say that when the separation distance between the fractures is upper to 65 km, fracture length well be independent.

In order to compare our results with geological field data, it is necessary to present a brief structural description of the Moroccan Atlas Mountain followed by a discussion. The installation of the Moroccan Atlas basin is controlled by the remobilization faults inherited from the Hercynian orogeny. Jacobshagen (1992) described two principal faults, the South Atlas Fault (SAF) NE-SW to E-W and the Translaboran Fault (TAF) trending NE-SW. Piqué & Laville (1993) describe two Paleozoic faults responsible of the Atlasic basin installation, they are Transforming Paleozoic Zone of Atlas (TPZA) trending E-W and Eastern Moroccan Orogenic Belt (EMOB) trending NE-SW.

Those faults are reactivated during the opening stage of the Atlasic basin from upper Permian to Triassic age; this event is related to the opening of the central Atlantic Ocean in one side and the new Tethys in the other side. The tectonic inversion of the Moroccan Atlas Mountain is related to the Africa-Eurasia convergence, the uprising stage of the Atlas is characterized by a structural context controlled by multiple relay on left lateral fault trending EW and NE-SW since the Bathonian age (Laville & Fedan, 1989). The major stage of tightening and the uprising relief are beginning from the Eocene-Paleocene age and continued during Miocene (Frizon de Lamotte *et al.,* 2008). The main faults trending N70 to EW are described as main thrust faults of the Atlas belt.

In The other hand, the opening of the Atlasic basin by favoring an oblique extension on a major transfer fault trending N120 to WNW-ESE since Triassic-Jurassic age (El Kochri & Chorowics 1996). The structural inversion begins with NS compression since the Eocene. The NW-SE to N120 faults have been described elsewhere in the High Atlas as paleogeographic fault, namely Demnat fault at the east part of Atlas Mountain (Le Marec & Jenny 1980) and the Berthat fault at the north part of Midelt-Errachidia transect (Benammi & El Kochri 1998).

If we compare the direction lineaments to the faults described in the Atlas, the main directions of lineaments ENE-WSW and WNW-ESE are the most dominant; they could correspond to the major directions described in the paragraph above. They correspond to the direction of the anticline ridges as sinistral fault and probably inherited from the Hercynian basement.

The lineaments of NE-SW direction, with 20% of all the lineaments is an important direction, it would correspond to the anticlinal ridges trending NE-SW (Fig. 1). This direction was also described as the main direction in the Middle Atlas (Laville & Fedan 1989) and secondary direction in the High Atlas. The NW-SE lineaments, is the minor direction with 5% of the all lineaments.

Concerning the age of the fractures, the first three principal directions NE-SW, ENE-WSW and WNW-ESE, have been described in the literature as faults that controlled the sedimentation during the Trias and Lower Lias age (Bouchouata *et al.,* 1995; Frizon de Lamotte *et al*., 2008). Those faults are reactivated during the different phases of the Atlas structuration as reverse fault. However, the NW-SE direction, and some minor fault trending NE-SW appear younger than the others, they cut across the main structures and provokes torsion of the anticline ridges ending. They can considered in most cases as response of Jurassic cover to the NW-SE and NE-SW faults in the basement reactivated during the main phase of tightening of the Atlas (Paleocene Eocene) (Ibouh *et al*., 2001).

Conclusions

The use of remote sensing on the visible and infrared bands of Landsat TM image added to the geographic information system (GIS) have contributed widely to create the fractures map with a fairly high number of fractures compared to the existing geological and structural maps. Firstly, the digital processing of satellite images has given a significant contribution to complete structural map of the Imilchil-Tounfite area. It can be use as a guide for future filed company in this area.On the other hand, statistical and geostatistical studies of the Imilchil-Tounfite area fractures, allows explaining how the fault network is structured in this region. The new fault network, mapped by remote sensing, will help us to understand the regional hydrological system (Chuma *et al*. 2013; Masoud & Koike 2006).

Control and mapping fractures in the study area can be used also in mining and hydrogeological exploration in the Imilchil-Tounfite region. This final cartographic document is a good starting point for any work of rural engineering. It will serve in a project study for the establishment of structures engineering such as road, railway or inland waterways (bridges, tunnels), dam or any other project and construction necessitating recognition characteristic soil and subsurface.

ACKNOWLEDGMENTS

The authors would like to thank the anonymous reviewers for their comments and suggestions that improved the final manuscript of this work. They also like to thank the executive editor Jose-Maria Cebria for all communication efforts and the work for the publication of this paper.

"The Authors would like also to thank the Geosciences and Environment laboratory, the Department of Geology in the Faculty of Sciences and Techniques of Marrakesh, for supportin this work".

References

Amri, K.; Mahjoub, Y. & Guergour, L. (2011). Use of Landsat 7 ETM+ for lithological and structural mapping of Wadi Afara Heouine area (Tahifet–Central Hoggar, Algeria, Arabian Journal of Geosciences, 4 (7): 1273–1287. http://dx.doi.org/10.1007/s12517-010-0180-8

Aouragh, H.; Essahlaoui, A. & Ouali, A. (2012). Lineaments frequencies from Landsat ETM + of the Middle Atlas Plateau (Morocco). Research Journal of Earth Sciences, 4 (1): 23–29. http://dx.doi.org/10.5829/idosi.rjes.2012.4.1.1106

Benammi, M. & El Kochri, A. (1998). Ouverture du rift atlasique: mise en évidence d'une paléofaille de transfert orientée N120. Comptes Rendus de l'Académie des Sciences - Series IIA - Earth and Planetary Science, 327 (12): 845–850. http://dx.doi.org/10.1016/S1251-8050(99)80060-3

Bouchouata, A.; Canerot, J.; Souhel, A. & Alméras, Y. (1994). Stratigraphie séquentielle et évolution géodynamique du Jurassique dans la région de Talmest-Tazoult (Haut Atlas Central). Comptes rendus de l'Académie des sciences. Série 2. Sciences de la terre et des planètes, T. 320: 749–756.

Bougadir, B. & Bouabdelli, M. (1994). Contribution to the cinematic introduction of plutons in the tectonic instability of the Aalenian and Bajocian ridges Tassent, Tazoult, Tassraft and Terrhist-Anefgou. Miscellanea del Servizio Geologico Nazionale (Roma), 5: 285–292.

Castaing, C.; Dutartre, P. & Fourniguet, J. (1988). Application of geological and structural criterion hydrogeological exploration in the base. BRGM: 1–48.

Chiles, J.P. (1998). Fractal and geostatistical methods for modeling of a fracture network. Mathematical Geology, 20 (6): 631–654. http://dx.doi.org/10.1007/BF00890581

Chuma, C.; Orimoogunje, O.I.; Hlatywayo, D.J. & Akinyede, J.O. (2013). Application of remote sensing and geographical information systems in determining the Ground water Potential in the Crystallin Basement of Bulwayo Metropolitan Area, Zimbabwe. Advances in Remote Sensing, 2 (2): 149–161. http://dx.doi.org/10.4236/ars.2013.22019

Diggle, P. & Ribeiro, P. (2007). Model-based Geostatistics. Springer, New York, 232 p. http://dx.doi.org/10.1007/978-0-387-48536-2

El Kochri, A. & Chorowics, J. (1996). Oblique extension in the Jurassic trough of the central and eastern High Atlas (Morocco). Canadian Journal of Earth Sciences, 33 (1): 84–92. http://dx.doi.org/10.1139/e96-009

Fadile, A. (2003). Carte géologique du Maroc au 1/100 000, feuille d'Imilchil. Notes et Mémoires du Service Géologique du Maroc, 397.

Frizon de Lamotte, D.; Zizi, M. & Missenard, Y. (2008). The Atlas System. In: Michard, A.; Saddiqi, O.; Chalouan, A. & Frizon de Lamotte, D. (Eds). Continental evolution: The Geology of Morocco. Springer: 133–202. http://dx.doi.org/10.1007/978-3-540-77076-3_4

Gringarten, E. & Deutsch, V. (2001). Teacher's Aide Variogram Interpretation and modeling.

Mathematical Geology, 33 (4): 507–534. http://dx.doi.org/10.1023/A:1011093014141

Hung, L.Q. & Batelaan, O.F. (2005). Lineament extraction and analysis, comparison of Landsat ETM and ASTER imagery: Case study: Suoimuoi tropical karst catchment, Vietnam. Proceedings SPIE 5983: Remote Sensing for Environmental Monitoring, GIS Applications, and Geology, V: 59830T. http://dx.doi.org/10.1117/12.627699

Ibouh, H. (1995). Tectonique en décrochement et intrusions magmatiques au Jurassique: tectogenèse polyphasée des rides jurassiques d'Imilchil (Haut Atlas central, Maroc). Thèse de 3ème cycle, Université Cadi Ayyad, Marrakech, 225 p.

Ibouh, H.; Bouabdelli, M. & Zargouni, F. (1994). Indices de tectonique synsédimentaire dans les dépôts aaléno-bajociens de la région d'Imilchil (Haut Atlas Central, Maroc). Miscellanea del Servizio Geologico Nazionale (Roma), 5: 305–310.

Ibouh, H.; El Bchari, F.; Bouabdelli, M.; Souhel, A. & Youbi, N. E. (2001). L'accident Tizal-Azourki: Haut Atlas central (Maroc). Manifestations synsédimentaires liasiques en extension et conséquence du serrage atlasique. Estudios Geológicos, 57 (1–2): 15–30. http://dx.doi.org/10.3989/egeol.01571-2124

Ibouh, H.; Michard, A.; Charriere, A.; Ben Kaddour, A.; & Ahoujjati, A. (2014). Tectonic–karstic origin of the alleged "impact crater" of Lake Isli (Imilchil district, High Atlas, Morocco). Comptes Rendus Geoscience, 346 (3–4): 82–89. http://dx.doi.org/10.1016/j.crte.2014.03.005

Jacobshagen, V. (1992). Major fracture zones of Morocco: The South Atlas and the Translaboran fault systems. Geologische Rundschau, 81 (1): 185–197. http://dx.doi.org/10.1007/BF01764548

Kassou, A.; Essahlaoui, A. & Aissa, M. (2012). Extraction of Structural Lineaments from Satellite Images Landsat 7 ETM+ of Tighza Mining District (Central Morocco). Research Journal of Earth Sciences, 4 (2): 44–48. http://dx.doi.org/10.5829/idosi.rjes.2012.4.2.1110

Katsuaki, K. & Yuichi, I. (2006). Spatial correlation structures of fracture systems for deriving a scaling law and modeling fracture distributions. Computers & Geosciences, 32 (8): 1079–1095. http://dx.doi.org/10.1016/j.cageo.2006.02.013

Kavac, K.S. (2005). Determination of palaeotectonic and neotectonic features around the Menderes Massif and the Gediz Graben (western Turkey) using Landsat TM image. International Journal of Remote Sensing, 26 (1): 59–78. http://dx.doi.org/10.1080/01431160410001709994

Koike, K. & Komorida, I.Y. (2001). Fracture-distribution modeling in rock mass using borehole data and geostatistical simulation. Proceedings of International Association for Mathematical Geology Conference, IAMG, Cancun, Mexico.

Laville, E. (1988). A multiples releasing and restraining stepover model for the Jurassic strike-slip basin of the Central High Atlas (Morocco). Developments in Geotectonics, 22 (1): 499–523. http://dx.doi.org/10.1016/B978-0-444-42903-2.50026-9

Laville, E. & Fedan, B. (1989). Le système atlasique marocain au Jurassique: évolution structurale et cadre géodynamique. Sciences Géologiques. Memoire, 84: 3–28.

Le Marec, A. & Jenny, J. (1980). L'accident de Demnat comportement synsédimentaire et tectonique d'un décrochement transversal du Haut Atlas Central (Maroc). Bulletin de la Société Géologique de France, S7-XXII (3): 421–427. http://dx.doi.org/10.2113/gssgfbull.S7-XXII.3.421

Masoud, A. & Koike, K. (2006). Tectonic architecture through Landsat-7 ETM+/SRTM DEM-derived lineaments and relationship to the hydrogeologic setting in Siwa region, NW Egypt. Journal African of Earth Sciences 45 (4–5): 467–477. http://dx.doi.org/10.1016/j.jafrearsci.2006.04.005

Michard, A.; Ibouh, H. & Charrière, A. (2011). Syncline-topped anticlinal ridges (STARs) from the High Atlas: a Moroccan conundrum, and inspiring structures from the Syrian Arc, Israel. Terra Nova, 23: 314–323. http://dx.doi.org/10.1111/j.1365-3121.2011.01016.x

Pepe, M.; Colombo, R. & Zilioli, E. (1997). Contribution of lineament pattern analysis from Landsat TM data to a geomophological-structural study of the Alpine-Dinaric domain. Proceedings SPIE 3222: Earth Surface Remote Sensing, 307. http://dx.doi.org/10.1117/12.298156

Piqué, A. & Laville, E. (1993). L'ouverture Atlantique Central : un rejeu en extension des structures paléozoïques. Comptes Rendus de l'Académie des Sciences de Paris, T.317: 1325–1332.

Qari, M.H.T. (2011). Lineament extraction from multi-resolution satellite imagery: a pilot study on Wadi Bani Malik, Jeddah, Kingdom of Saudi Arabia. Arabian Journal of Geosciences, 4 (7): 1363–1371. http://dx.doi.org/10.1007/s12517-009-0116-3

Semere, S. & Woldi, G. (2006). Lineament characterization and their tectonic significance using Landsat TM data and field studies in the central highlands of Eritrea. Journal of African of Earth Sciences 46 (4): 371–378. http://dx.doi.org/10.1016/j.jafrearsci.2006.06.007

Singh, A. & Harrison, A. (1985). Standardized principal components. International Journal of Remote Sensing, 6 (6): 883–896. http://dx.doi.org/10.1080/01431168508948511